Li *et al*. *Complex Eng Syst* 2024;4:5
DOI: 10.20517/ces.2023.38

Complex Engineering Systems

Research Article

Open Access

Check for updates

Command filter-based adaptive neural tracking control of nonlinear systems with multiple actuator constraints and disturbances

Yinguang Li, Jianhua Zhang, Yang Li

School of Information and Control Engineering, Qingdao University of Technology, Qingdao 266520, Shandong, China.

Correspondence to: Dr. Jianhua Zhang, School of Information and Control Engineering, Qingdao University of Technology, No. 777, East Jialingjiang Road, Huangdao District, Qingdao 266520, Shandong, China. E-mail: Jianhuazhang@qut.edu.cn

How to cite this article: Li Y, Zhang J, Li Y. Command filter-based adaptive neural tracking control of nonlinear systems with multiple actuator constraints and disturbances. *Complex Eng Syst* 2024;4:5. http://dx.doi.org/10.20517/ces.2023.38

Received: 16 Oct 2023 **First Decision:** 7 Dec 2023 **Revised:** 5 Jan 2024 **Accepted:** 15 Jan 2024 **Published:** 21 Feb 2024

Academic Editors: Yurong Liu, Hamid Reza Karimi **Copy Editor:** Fangling Lan **Production Editor:** Fangling Lan

Abstract

In this paper, the adaptive practical finite-time tracking control problem for a class of strictly feedback nonlinear systems with multiple actuator constraints is investigated using backstepping techniques and practical finite-time stability theory. The effects of deadband and saturated nonlinear constraints on the controller design of nonlinear systems are addressed by the equivalent transformation method. The problem of complexity explosion due to the derivatives of virtual control signals is solved by using the virtual control signals as inputs to the command filters and using the outputs of the command filters to perform the corresponding control tasks. An adaptive neural network tracking backstepping control strategy based on the command filter technique and the backstepping design algorithm is proposed by approximating an unknown nonlinear function using a neural network. The control strategy ensures the boundedness of all variables in the closed-loop system, and the output tracking error fluctuates in a small region near the origin. Finally, simulations verify the effectiveness of the control strategy designed in this paper.

Keywords: Nonlinear systems, actuator constraint, command filtering, neural network, adaptive

1. INTRODUCTION

The control theory of nonlinear systems has been widely developed in the past two decades, and how to design controllers that are more reasonable and meaningful for nonlinear systems has gradually become an active topic, such as the design of tracking control for nonlinear systems[1–4]. The backstepping method is a practical approach to nonlinear control problems and was proposed by Kanellakopoulos *et al*. at the end of the last century[5]. Combining the backstepping method with the fuzzy or neural adaptive technique yields an effective control tool for solving uncertain nonlinear systems[6]. Due to the Characteristics of the adaptive backstepping method, it is possible to achieve asymptotic sedimentation of nonlinear systems and guarantee boundedness of the signal under parameter uncertainty, which has led to many fruitful results[7–9]. The adaptive neural fault-tolerant decentralized tracking control problem for switching stochastic uncertain nonlinear systems has been studied in the literature[10]. The article[11] investigates the design of discounted iterative adaptive critic for tracking control of affine nonlinear systems by introducing a new cost function. The authors[12] investigate the output consensus control of heterogeneous multiagent systems (MASs) by designing a distributed adaptive observer for each follower and introducing an additional tracking error observer. The article[13] deals with the attitude and vibration problems of flexible spacecraft simultaneously by proposing a novel adaptive control strategy. In the literature[14], adaptive tracking control of nonlinear systems with unknown input constraints and unpredictable variables is studied. In the literature[15], a controller design strategy based on separation of variables is designed for non-strict feedback nonlinear systems. The neural adaptive FTC technique allows the controlled system to achieve good tracking performance in finite time, and the whole variables of the closed-loop system are bounded[16]. The article[17] addresses the problem of finite-time control of non-triangular uncertain stochastic nonlinear systems. The authors[18] investigate adaptive finite-time control for nonlinear systems with input quantization and full-state constraints.

Although the fuzzy/neural adaptive inversion algorithm is one of the most general methods for controller design of nonlinear systems and has solved many problems in the field of control[19]. However, it should be noted that since the virtual control inputs in the controller design process need to be differentiated and iterated repeatedly, the design of controllers for nonlinear systems using adaptive inversion algorithms will become more and more computationally intensive along with the increase in the order of the system, a phenomenon we refer to as ”complexity explosion”[20]. In order to solve the defect of ”complexity explosion” of traditional backstepping algorithms, two methods of dynamic surface control (DSC)[21] and command filter backstepping control[22] have emerged. However, as DSC ignores the errors introduced by the filter, it affects the control accuracy of the controlled system[23]. Since then, the backstepping command filtering method has been combined with the adaptive technique to achieve significant results in eliminating the filter errors[24,25]. The article[26] investigates the work on life prediction of lithium-ion batteries using adaptive techniques and filtering methods. In this article, the problem of tracking control of uncertain higher-order nonlinear systems with input saturation is investigated based on the command filtering technique[27].

Compared with asymptotic sedimentation methods, finite-time control methods have the advantages of fast convergence, high accuracy, good performance, and robustness to uncertainty and have achieved fruitful results[28]. In practical engineering applications, nonlinear problems, such as hysteresis, deadband, saturation, and external disturbances, often occur. Deadband and saturation, as non-smooth functions, have a large impact on system control performance. Therefore, special attention should be paid to the controller design process of nonlinear systems. Li *et al*. combined the obstacle Lyapunov function with an adaptive backstepping control method to solve a FTC problem for nonlinear systems with dead zones[29]. In recent years, many effective results have emerged for nonlinear systems with different input constraints[30,31]. However, to our knowledge, few research results use a combination of neural adaption and command filtering to solve simultaneous input deadband, saturation, and nonlinear disturbances. Therefore, it is an interesting task to study finite-time stabilized controllers for nonlinear systems with simultaneous multiple input constraints and Nonlinear disturbances.

In summary, it can be seen that external disturbances and the presence of input constraints on the actuator can have a significant impact on system control performance and safety, especially in control processes, such as Mars drones far from Earth and chemical reactions with major safety incidents. Therefore, in this paper, for a class of uncertain nonlinear systems with multiple actuator constraints and external disturbances, a practical adaptive neural network (NN) FTC method is designed to reduce the effects of actuators and disturbances on the tracking performance of the system. Compared with the current research results, the main contributions can be summarized as follows:

1: In this paper, the problem of adaptive NN backstepping control for nonlinear systems with multiple actuator constraints and external disturbances is investigated by combining neural adaptive and command filtering techniques. Under the combined influence of multiple actuator constraints and external disturbances, the controller design task is accomplished, and good tracking control performance is achieved.

2: The use of command filtering and compensation mechanisms solves the complexity explosion problem while eliminating the effect of filtering errors. Deadband and saturation are grouped into one model, simplifying the difficult problem of designing controllers under multiple constraints.

3: With the control method used in this paper, all signals of the controlled system are bounded, which meets the realistic requirements of the actual physical control process, and the output tracking error can be quickly converged to within a bounded and adjustable tight set in finite time.

The rest of this paper is described below. Section 2 provides an introduction to the problem description and preparatory knowledge. Section 3 presents the controller design and stability analysis of the adaptive NN tracking control. Section 4 gives the numerical simulations and the result analysis. Finally, Section 5 analyzes and concludes the paper.

2. PROBLEM FORMULATION AND PRELIMINARIES

In this section, the system model and NN and preparatory knowledge are described. For convenience, the following notations are used in this paper. $|*|$ represents the absolute value of $*$. $y^{(j)}$ is the j-order differentiation of y. x^T denotes the transpose of matrix x. R^n and $R^{n\times n}$ denote the n-dimensional Euclidean space and the real $n \times n$-matrix spaces, respectively. Ω_Z represents the compact set.

2.1. System model

Consider the following strictly feedback nonlinear system [32].

$$\begin{cases} \dot{x}_i = x_{i+1} + f_i(\bar{x}_i) + d_i(t), 1 \le i \le n-1, \\ \dot{x}_n = u(t) + f_n(\bar{x}_n) + d_n(t), \\ y = x_1 \end{cases} \tag{1}$$

in which $\bar{x}_i = [x_1(t), \dots, x_i(t)]^T \in R^n, i = 1, \dots, n$ expresses the system state variables, and y indicates the system output; $f_i(\bar{x}), i = 1, \dots, n$ displays the unknown smooth nonlinear functions. $d_i(t)$ represents unknown bounded external interference with $x_{i+1} + f_i(x) \neq 0$. $u(t)$ represents control inputs subject to nonlinearities of multiple actuator constraints and is described as

$$u = m(v)v + \pi(v) \tag{2}$$

where v represents the input signal for dead zone and saturation nonlinear models. Select l_+, l_-, u_+, u_- as positive design constants, and $u_H > 0 and u_L > 0$ denote the normal number to be designed. $m(v)$ called the dead zone slope, and $m(v), \pi(v)$ are expressed by

$$m(v) = \begin{cases} \frac{u_H}{v}, v > u_H \\ l_+,\ u_+ < v < u_H \\ l_+,\ \ -u_- < v < u_+ \\ l_-,\ \ -u_L < v < u_- \\ -\frac{u_L}{v}, v < -u_L \end{cases} \tag{3}$$

$$\pi(v) = \begin{cases} 0, v > u_H \\ -l_+u_+, u_+ < v < u_H \\ -l_+v,\ \ -u_- < v < u_+ \\ -l_-u_-, -u_L < v < u_- \\ 0, v < -u_L \end{cases} \tag{4}$$

2.2. Mathematical preparation

The objective of this paper is to design a new finite-time tracking control algorithm for nonlinear systems with tight feedback so that the system output can trace the wanted trajectory signal in finite time and all the variables of the considered system are well bounded, so the below assumptions and lemmas are implemented without loss of generality.

Assumption 1:[33] The positive and negative slopes of the dead zone and saturation nonlinear models are equal; i.e., $l_+ = l_- = l$. Dead-zone parameters of the controller, u_+, u_-, and l, are bounded; that is, there are known parameters $u_{+\max}, u_{-\max}$, and $l_{\max}$ that $|u_+| < u_{+\max}, |u_-| < u_{-\max}$, and $|l| < l_{\max}$.

Remark 1: In real production process environments, special requirements are usually imposed on the inputs to the system actuators, such as controlling the maximum amplitude of the inputs within a certain range and avoiding fluctuations near zero as much as possible in order to minimize the consumption. Deadband and saturation constraints are direct manifestations of the above problems in real physical systems. In order to place limits on the control inputs and retain the control capability of the controller, the parameters associated with the deadband and saturation models must be bounded; otherwise, the controller will lose its control capability. For example, if u_+, u_- is infinite, the control input is always in the dead zone, and the ability to control is disabled. From Assumption 1, It is not difficult to obtain that $\pi(v)$ is bounded, and $|\pi(v)| \le D$, in which D represents the upper limit value.

Assumption 2:[34] The anticipated tracking trace signal y_d and its first derivative considered in this paper are continuous and bounded.

Remark 2: Consider the actual situation; the control input signal v cannot be infinite. Therefore, consider that $m(v)$ satisfies the following inequality

$$0 < \gamma \le \min\left\{\frac{u_H}{v_{\max}}, l\right\} \le m(v) \le \max\{1, l\} \tag{5}$$

in which $v_{\max}$ represents the maximum value of the designed controller.

Lemma 1:[35] In this paper, RBF NNs will be utilized to approximate unknown nonlinear functions. For a continuous function $h(Z)$, there exists that

$$h_i(Z) = \phi_i^T R_i(x) + \delta_i(x) \tag{6}$$

where $Z \in \Omega_Z \subset R^n$ denotes the input vector, $\phi = [\phi_1, \phi_2, \ldots, \phi_m]^T \subset R^m$ expresses the ideal weight vectors, in which $m > 1$ is the NN node number. $\delta(x)$ indicates the approaching error, and $R(Z) = [R_1(Z), R_2(Z), \ldots, R_m(Z)]^T$ represents the vectors of RBF basis functions.

Lemma 2:[36] The filters used in this paper are described as follows

$$\begin{cases} \dot{\omega}_i = \omega_\tau \omega_{i,2} \\ \dot{\omega}_{i,2} = -2\varsigma\omega_\tau\omega_{i,2} - \omega_\tau(\dot{\omega}_i - \alpha_{i-1}) \end{cases} \tag{7}$$

where $\varsigma \in (0, 1]$ and $\omega_\tau > 0$ indicate positive filter parameters. Consider Virtual Controller α_{i-1} and ω_i as input and output of the filter, respectively, in which $\omega_i(0) = \alpha_{i-1}(0), \omega_{i,2}(0) = 0$.

Remark 3: In the process of designing a controller using the backstepping method, the computational burden of the controller design increases dramatically with the system scale due to the repeated differentiation of the virtual control inputs. In order to overcome this complexity explosion, this paper uses the command filtering technique to perform filtering operations on the virtual control signals in order to eliminate the repetitive differentiation of the virtual control signals. The virtual control signal is used as the input to the command filter, and a good filtered output signal can be obtained by adjusting the ω_τ and ς parameters. In order to demonstrate the effect of the command filter parameters on the filtered output, the output of the command filter is plotted compared to the trajectory of the input signal using the following three different sets of filter parameters (1) ω_1 ($\omega_\tau = 60, \varsigma = 0.85$); (2) ω_2 ($\omega_\tau = 20, \varsigma = 0.85$); (3) ω_3 ($\omega_\tau = 60, \varsigma = 0.2$), which are displayed in Figure 1. Figure 1 illustrates the filtered output traces corresponding to different filter parameters. It can be seen that parameter ω_τ affects the tracking error of the filtered output, and parameter ς affects the tracking performance in the pre-period.

Lemma 3:[37] For any positive constants b_1, b_2, b_3 and real variables x, y, the below inequality holds

$$|x|^{b_1}|y|^{b_2} \leq \frac{b_1}{b_1 + b_2} b_3 |x|^{b_1+b_2} + \frac{b_2}{b_1 + b_2} b_3^{-\frac{b_1}{b_2}} |y|^{b_1+b_2} \tag{8}$$

Lemma 4:[38] Consider a dynamic system $\dot{x} = f(x, u), x(t_0) = x_0$, in which $f : R^n \to R^n$ represents a smooth mapping. If there exists a Radically unbounded and deterministic positive scalar function $V(x)$, $\mu_1 > 0, \mu_1 > 0$ and $0 < q < 1, 0 < \delta < \infty$ such that

$$\dot{V}(x, t) \leq -\mu_1 V(x) - \mu_2 V^q(x) + \delta \tag{9}$$

Then, the output of this system $\dot{x} = f(x, u)$ is practical finite-time stable, and the set of residuals of the system solution is shown below

$$\lim_{t\to T_r} V(x) \leq \min\left\{\frac{\sigma}{(1-\varphi)\alpha}, (\frac{\sigma}{(1-\varphi)\beta})^{\frac{1}{q}}\right\} \tag{10}$$

in which $\varphi \in (0,1)$. Then, one can obtain the settling time bounded by

$$\begin{aligned} T_r \leq \max\Bigg\{ & t_0 + \frac{1}{\varphi\mu_1(1-q)} \ln \frac{\varphi\mu_1 V^{1-q}(t_0) + \mu_2}{\mu_2}, \\ & t_0 + \frac{1}{\mu_1(1-q)} \ln \frac{\mu_1 V^{1-q}(t_0) + \varphi\mu_2}{\varphi\mu_2}\Bigg\} \end{aligned} \tag{11}$$

Remark 4: The above Lemma 4 gives a practical finite-time stability criterion for nonlinear systems. Next, this paper will use Lemma 4 as a basis for designing command-filtered adaptive NN tracking controllers for strict-feedback nonlinear systems with dead-zone and saturation constraints.

3. CONTROLLER DESIGN AND STABILITY ANALYSIS

3.1. Finite-time controller design

In this subsection, an adaptive NN controller will be designed for system 1 by backstepping algorithms. The controller will handle both the tracking performance of the system and the boundedness of the variables. Moreover, the complexity explosion of the classical backstepping algorithm is conquered by the command filtering method. The controller consists of some basic stages, and the design is built on the following coordinate transformation

$$\begin{cases} z_1 = x_1 - y_d \\ z_i = x_i - \omega_i \end{cases} \tag{12}$$

in which y_d expresses the desired reference trajectory signal, and ω_i with $i = 2, 3, \ldots, n$ represents the introduced command filter variable.

Remark 5: Note that the command filter will increase the operational burden of the actuator due to the error defect introduced. To address this drawback, a compensation signal will be designed to compensate for the tracking error $(\omega_i - \alpha_{i-1})$ incurred by the command filter.

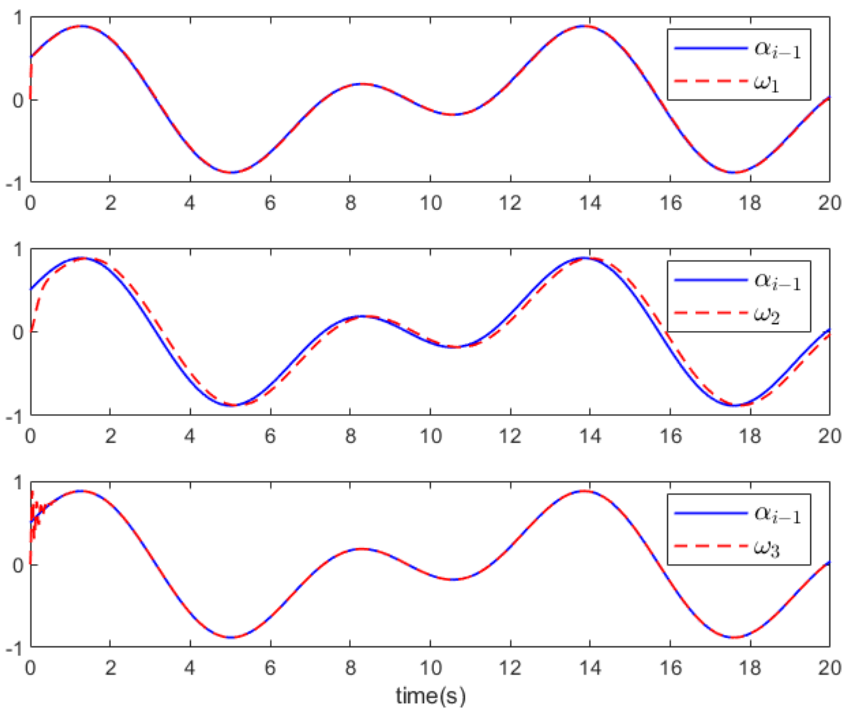

Figure 1. Command filter output.

In addition, in order to reduce the computation of controller design, the following compensation tracking error is constructed based on the idea of coordinate transformation:

$$\xi_i = z_i - r_i, i = 1, \ldots, n \tag{13}$$

where r_i indicates the compensated signal.

Step 1: With the aid of (1), (12), and (13), the following equation can be obtained

$$\dot{\xi}_1 = \xi_2 + r_2 + \omega_2 + f_1 + d_1 - \dot{y}_d - \dot{r}_1 \tag{14}$$

Select a Lyapunov function V_1 as

$$V_1 = \frac{1}{2}\xi_1^2 + \frac{1}{2\lambda_1}\tilde{\theta}_1^2 \tag{15}$$

where $\lambda_1 = 2\rho_1/(2\rho_1 - 1), \rho_1 > 1/2$ denotes the parameters to be constructed. $\tilde{\theta}_1 = \theta_1 - \hat{\theta}_1$, in which $\hat{\theta}_1$ denotes the estimate of the uncertain parameter θ_1.

Taking the time derivative of V_1, for $\forall q \in \left(\frac{1}{2}, 1\right)$, it follows that

$$\dot{V}_1 = \xi_1(-k_{1,2}\xi_1^{2q-1} + \xi_2 + r_2 + \omega_2 + h_1(Z_1) - \dot{r}_1 - \dot{y}_d) - \frac{1}{\lambda_1}\tilde{\theta}_1\dot{\hat{\theta}}_1 \tag{16}$$

where $h_1(Z_1) = f_1 + d_1 + k_{1,2}\xi_1^{2q-1}$ is not available for feedback due to the existence of unknown nonlinear functions. Then, $h_1(Z_1)$ will be approximated by RBF NNs as

$$h_1(Z_1) = \phi_1{}^{*T}R_1(x) + \delta_1(x),, \quad |\delta_1(\zeta_1)| \le \varepsilon_1 \tag{17}$$

where $Z_1 = [x_1, y_d, \dot{y}_d]^T$, and $\delta_1(Z_1)$ represents the estimate error, with arbitrary constants $\varepsilon_1 > 0$. Applying Young's inequality, it produces

$$\xi_1 h_1(Z_1) \leq \frac{1}{2a_1^2}\xi_1^2\theta_1 R_1^T R_1 + \frac{a_1^2}{2} + \frac{1}{2}\xi_1^2 + \frac{1}{2}\varepsilon_1^2 \tag{18}$$

where $\theta_1 = \left\|\phi_1^*\right\|^2, a_1 > 0$.

Next, the virtual controller is introduced as α_1, and a compensating signal r_1 is designed as

$$\alpha_1 = -k_{1,1}z_1 - \frac{1}{2a_1^2}\xi_1\hat{\theta}_1 R_1^T R_1 - \frac{1}{2}\xi_1 + \dot{y}_d \tag{19}$$

$$\dot{r}_1 = -k_{1,1}r_1 + r_2 + \omega_2 - \alpha_1 \tag{20}$$

where $k_{1,1}$ indicates a parameter to be built.

With the aid of (17)–(20), the following inequality holds

$$\dot{V}_1 \leq -k_{1,1}\xi_1^2 - k_{1,2}\xi_1^{2q} + \frac{\tilde{\theta}_1}{\lambda_1}(\frac{\lambda_1}{2a_1^2}\xi_1^2 R_1^T R_1 - \dot{\hat{\theta}}_1) + \xi_1\xi_2 + \frac{1}{2}a_1^2 + \frac{1}{2}\varepsilon_1^2 \tag{21}$$

Then, building an adaptive law $\dot{\hat{\theta}}_1$ as

$$\dot{\hat{\theta}}_1 = \frac{\lambda_1}{2a_1^2}\xi_1^2 R_1^T R_1 - \eta_1\hat{\theta}_1 \tag{22}$$

Thus, on the basis of the above equation, the following inequality holds

$$\dot{V}_1 \leq -k_{1,1}\xi_1^2 - k_{1,2}\xi_1^{2q} + \frac{\eta_1}{\lambda_1}\tilde{\theta}_1\hat{\theta}_1 + \xi_1\xi_2 + \frac{1}{2}a_1^2 + \frac{1}{2}\varepsilon_1^2 \tag{23}$$

Step i: With the aid of (1), (12), and (13), similar to step 1 as

$$\dot{\xi}_i = \xi_{i+1} + r_{i+1} + \omega_{i+1} + f_i + d_i - \dot{\omega}_i - \dot{r}_i \tag{24}$$

Select a Lyapunov function V_i as

$$V_i = V_{i-1} + \frac{1}{2}\xi_i^2 + \frac{1}{2\lambda_i}\tilde{\theta}_i^2 \tag{25}$$

where $\lambda_i = 2\rho_i/(2\rho_i - 1), \rho_i > 1/2$ represents a parameter to be constructed.

Then, similarly to step 1, the following inequality holds

$$\begin{aligned}\dot{V}_i \leq & -\sum_{j=1}^{i-1} k_{j,1}\xi_1^2 - \sum_{j=1}^{i-1} k_{j,2}\xi_1^{2q} + \sum_{j=1}^{i-1}\frac{\eta_j}{\lambda_j}\tilde{\theta}_j\hat{\theta}_j + \xi_i(\xi_{i-1} - k_{i,2}\xi_i^{2q-1} + \xi_{i+1} + r_{i+1} + \omega_{i+1} \\ & + h_i(Z_i) - \dot{r}_i - \dot{\omega}_i) - \frac{1}{\lambda_i}\tilde{\theta}_i\dot{\hat{\theta}}_i - \frac{1}{2}\xi_i^2 + \frac{1}{2}\sum_{j=1}^{i-1}(a_j^2 + \varepsilon_j^2)\end{aligned} \tag{26}$$

in which $h_i(Z_i) = f_i + d_i + k_{i,2}\xi_i^{2q-1} - \xi_{i-1}$. Similarly, there exists NNs and $\forall\varepsilon_i > 0$. Consequently, $h_i(Z_i) = \phi_i^{*T} R_i(x) + \delta_i(x)$ with $|\delta_i(Z_i)| \le \varepsilon_i$.

Combining Young's inequality, the following inequality holds

$$\xi_i h_i(Z_i) \le \frac{1}{2a_i^2}\xi_i^2\theta_i R_i^T R_i + \frac{a_i^2}{2} + \frac{1}{2}\xi_i^2 + \frac{1}{2}\varepsilon_i^2 \tag{27}$$

where $\theta_i = \left\|\phi_i^*\right\|^2, a_i > 0$.

Next, the virtual controller is introduced as α_1, and the compensating signal is constructed as $\dot{r}_1$, along with the adaptive law $\dot{\hat{\theta}}_i$, as follows:

$$\alpha_i = -k_{i,1}z_i - \frac{1}{2}\xi_i - \frac{1}{2a_i^2}\xi_i\hat{\theta}_i R_i^T R_i + \dot{\omega}_i \tag{28}$$

$$\dot{r}_i = -k_{i,1}r_i + r_{i+1} + \omega_{i+1} - \alpha_i \tag{29}$$

$$\dot{\hat{\theta}}_i = \frac{\lambda_i}{2a_i^2}\xi_i^2 R_i^T R_i - \eta_i\hat{\theta}_i \tag{30}$$

where $k_{i,1}$ indicates a normal number to be constructed. With the help of (27)–(30), the following inequality holds

$$\dot{V}_i \le -\sum_{j=1}^{i} k_{j,1}\xi_1^2 - \sum_{j=1}^{i} k_{j,2}\xi_1^{2q} + \sum_{j=1}^{i}\frac{\eta_j}{\lambda_j}\tilde{\theta}_j\hat{\theta}_j + \frac{1}{2}\sum_{j=1}^{i}(a_j^2 + \varepsilon_j^2) + \xi_i\xi_{i+1} \tag{31}$$

Step n: With the aid of (1), (12), and (13), one can get the derivative of ξ_n as

$$\dot{\xi}_n = u(t) + f_n - \dot{\omega}_n - \dot{r}_n + d_n = m(v) + \pi(v) + f_n + d_n - \dot{\omega}_n - \dot{r}_n \tag{32}$$

Select a Lyapunov function V_n as

$$V_n = V_{n-1} + \frac{1}{2}\xi_n^2 + \frac{1}{2\lambda_n}\tilde{\theta}_n^2 \tag{33}$$

Then, we obtain the $\dot{V}_i$ by (32) and (33) as:

$$\begin{aligned}\dot{V}_i \le & -\sum_{j=1}^{n-1} k_{j,1}\xi_1^2 - \sum_{j=1}^{n-1} k_{j,2}\xi_1^{2q} + \sum_{j=1}^{n-1}\frac{\eta_j}{\lambda_j}\tilde{\theta}_j\hat{\theta}_j + \xi_n(\xi_{n-1} - k_{n,2}\xi_n^{2q-1} + m(v)v + \pi(v) + h_n(Z_n) \\ & - \dot{\omega}_n - \dot{r}_n) - \frac{1}{\lambda_n}\tilde{\theta}_n\dot{\hat{\theta}}_n - \frac{1}{2}\xi_n^2 + \frac{1}{2}\sum_{j=1}^{n-1}(a_j^2 + \varepsilon_j^2)\end{aligned} \tag{34}$$

where $h_n(Z_n) = f_n + d_n + k_{n,2}\xi_n^{2q-1} - \xi_{n-1}$. Similar to (17) and (27), we can get

$$\xi_n h_n(Z_n) \le \frac{1}{2a_n^2}\xi_n^2\theta_n R_n^T R_n + \frac{a_n^2}{2} + \frac{1}{2}\xi_n^2 + \frac{1}{2}\varepsilon_n^2 \tag{35}$$

$$\xi_n\pi(v) \le \frac{1}{2}\xi_n^2 + \frac{1}{2}D^2 \tag{36}$$

where $|\pi(v)| < D$.

Now, as obtained from Remark 2, the actual control signal v, compensation signal $\dot{r}_n$, and adaptive law $\dot{\hat{\theta}}_n$ can be constructed as follows:

$$v = \frac{1}{\gamma}(-k_{n,1}z_n - \xi_n - \frac{1}{2a_n^2}\xi_n\hat{\theta}_n R_n^T R_n + \dot{\omega}_n) \tag{37}$$

$$\dot{r}_n = -k_{n,1}r_n \tag{38}$$

$$\dot{\hat{\theta}}_n = \frac{\lambda_n}{2a_n^2}\xi_n^2 R_n^T R_n - \eta_n\hat{\theta}_n \tag{39}$$

where $k_{n,1}$ indicates a normal number to be constructed. With the help of (35)–(39), the following inequality holds

$$\dot{V}_n \leq -\sum_{j=1}^{n} k_{j,1}\xi_1^2 - \sum_{j=1}^{n} k_{j,2}\xi_1^{2q} + \sum_{j=1}^{n}\frac{\eta_j}{\lambda_j}\tilde{\theta}_j\hat{\theta}_j + \frac{1}{2}\sum_{j=1}^{n}(a_j^2 + \varepsilon_j^2) + \frac{1}{2}D^2 \tag{40}$$

Algorithm 1 Proposed Control Algorithm

Initialize: $i = 1$, selecting the desired trajectory signal y_d
while $i \leq n$ **do**
  Choose the Lyapunov function V_i and derive it to obtain the derivative $\dot{V}_i$.
  Approximating the nonlinear function in $\dot{V}_i$ using RBF NNs.
  Constructing the virtual controller α_i or the final actual controller v.
  while $i < n$ **do**
    Take the virtual control signal α_{i-1} into the command filter to get the filtered output signal ω_i.
  end while
  Construct the compensation signal $\dot{r}_i$, which compensates for the filtering error due to the command filter.
  Choose the adaptive laws $\dot{\hat{\theta}}_i$.
end while
return α_i, v, $\dot{r}_i$, $\dot{\hat{\theta}}_i$.

3.2. Stability analysis

Now, after the above n-step controller design, the controller construction has been completed. This section will be concluded by the following theorem.

Theorem 1: For the uncertain nonlinear system (1) that meets the conditions of Assumptions 1 and 2, under adopting the controller (19), (28), (37) and the adaptive law (30), the controlled system is practically finite-time stable, and the signals of the system are bounded almost surely.

Proof: Recalling the definition $\tilde{\theta}_1 = \theta_1 - \hat{\theta}_1$, for any $\rho_j > 1/2$, the following inequality can be obtained

$$\tilde{\theta}_j\hat{\theta}_j \leq \frac{\rho_i}{2}\theta_j^2 - \frac{1}{\lambda_j}\tilde{\theta}_j^2 \tag{41}$$

With the aid of (41), yields

$$\begin{aligned}\dot{V}_n \leq & -\sum_{j=1}^{n} k_{j,1}\xi_1^2 - \sum_{j=1}^{n} k_{j,2}\xi_1^{2q} - \sum_{j=1}^{n} \frac{\eta_j}{2\lambda_j}\tilde{\theta}_j^2 - \sum_{j=1}^{n} \frac{\eta_j}{2\lambda_j}\tilde{\theta}_j^2 + \frac{1}{2}\sum_{j=1}^{n}(a_j^2 + \varepsilon_j^2 + \rho_j\eta_j\theta_j^2) + \frac{1}{2}D^2 \\ = & -a\sum_{j=1}^{n}\frac{1}{2}\xi_j^2 - a(\sum_{j=1}^{n}\frac{1}{2}\xi_j^2)^q - a\sum_{j=1}^{n}\frac{\tilde{\theta}_j^2}{2\lambda_j} - a(\sum_{j=1}^{n}\frac{\tilde{\theta}_j^2}{2\lambda_j})^q + \sum_{j=1}^{n}\eta_j(\frac{\tilde{\theta}_j^2}{2\lambda_j})^q - \sum_{j=1}^{n}\frac{\eta_j}{2\lambda_j}\tilde{\theta}_j^2 \\ & + \frac{1}{2}\sum_{j=1}^{n}(a_j^2 + \varepsilon_j^2 + \rho_j\eta_j\theta_j^2) + \frac{1}{2}D^2\end{aligned} \tag{42}$$

where $a = \min\left\{2k_{j,1}, 2^q k_{j,2}, \eta_j, j = 1, \dots, n\right\}$.

By applying Lemma 3, the following equation can be obtained

$$(\sum_{j=1}^{n}\frac{1}{2\lambda_j}\tilde{\theta}_j^2)^q \leq \sum_{j=1}^{n}\frac{1}{2\lambda_j}\tilde{\theta}_j^2 + (1-q)q^{\frac{q}{1-q}} \tag{43}$$

where $x = 1, y = \sum_{j=1}^{n}\frac{1}{2\lambda_j}\tilde{\theta}_j^2, b_1 = \frac{1}{4}, b_2 = \frac{3}{4}$.

With the aid of (41)-(43), the following equation can be obtained

$$\dot{V}_n \leq -\alpha V_n - \beta V_n^q + \delta_1 \tag{44}$$

in which $\alpha = \beta = a, \delta_1 = \frac{1}{2}\sum_{j=1}^{n}(a_j^2 + \varepsilon_j^2 + \rho_j\eta_j\theta_j^2) + \frac{1}{2}D^2 + (1-q)q^{\frac{q}{1-q}}$.

By using the formulation of Theorem 4, it can be easily obtained that the system (1) considered in this paper is practically finite-time stable and converges to the following compact set

$$\xi_i \in \min\left\{V(x) \leq \frac{\delta_1}{(1-\varphi)\alpha}, (\frac{\delta_1}{(1-\varphi)\beta})^{\frac{1}{q}}\right\} \tag{45}$$

where $\varphi \in (0, 1)$. Then, the upper limit of the settling time can be expressed as

$$\begin{aligned}T \leq T_r = \max\Bigg\{ & t_0 + \frac{1}{\varphi\alpha(1-q)}\ln\frac{\varphi\alpha V^{1-q}(t_0) + \beta}{\beta}, \\ & t_0 + \frac{1}{\alpha(1-q)}\ln\frac{\alpha V^{1-q}(t_0) + \varphi\beta}{\varphi\beta}\Bigg\}\end{aligned} \tag{46}$$

Since the boundedness of the error $\xi_i = z_i - r_i$ is closely related to z_i and r_i. Therefore, in order to obtain the convergence of z_i, the boundedness of r_i has to be considered. To demonstrate the convergence of the error compensation system, the Lyapunov function is constructed as follows

$$V_r = \frac{1}{2}\sum_{j=1}^{n} r_j^2 \tag{47}$$

According to (20), (29), and (38), the derivative of V_r is obtained as

$$\dot{V}_r = r_1\left(-k_{1,1}r_1 + r_2 + (\omega_2 - \alpha_1)\right) + r_2\left(-k_{2,1}r_2 + r_3 + (\omega_3 - \alpha_2)\right) + \cdots + r_n\left(-k_{n,1}r_n\right) \tag{48}$$

Based on Young's inequality, it yields

$$r_j r_{j+1} \leq \frac{1}{2} r_j^2 + \frac{1}{2} r_{j+1}^2 \tag{49}$$

$$r_j \left(\omega_{j+1} - \alpha_j\right) \leq \frac{1}{2\eta} r_j^2 + \frac{\eta}{2} H_j^2 \tag{50}$$

where η is a positive constant, and H satisfies $\left|\omega_{j+1} - \alpha_j\right| \leq H_j$. Substituting (49) and (50) into (48) yields

$$\dot{V}_r \leq -\sum_{j=1}^{n} \kappa r_j^2 + \frac{n-1}{2} \eta H^2 \leq -\frac{\kappa}{2} V_r^2 + \frac{n-1}{2} \eta H^2 \tag{51}$$

in which $\kappa = \min\left\{k_{j,1} - \frac{1}{2} - \frac{1}{2\eta}\right\}$, $H = \max\left\{\sqrt{\eta} H_j\right\}$. Thus, from Gronwall's Lemma, it follows that

$$0 \leq V_r \leq \left(V_r(0) - \frac{(n-1)\eta H^2}{\kappa}\right) e^{-\frac{\kappa}{2}t} + \frac{(n-1)\eta H^2}{\kappa} \tag{52}$$

From the above discussion, it can be concluded that $\xi_i, \tilde{\theta}_i$, and r_i are bounded. Because $\hat{\theta}_i$ denotes the estimate of the uncertain parameter θ_i and $\tilde{\theta} = \theta - \hat{\theta}$, one has $\hat{\theta}_i$ is bounded. From the definition of the compensation error $\xi_i = z_i - r_i$, it follows that z_i is bounded. From (19) and (28), it follows that α_i are bounded because they are composed of $z_i, \xi_i, \hat{\theta}_i$. Since α_i is bounded, ω_i must also be bounded. Thus, by the definition of the tracking error $z_i = x_i - \omega_i$, x_i is also bounded. The boundedness of the controller can be deduced, too. Thus, we prove the boundedness of all closed-loop signals of the system.

By the above description, it is proven to be completed. For a clearer understanding of the controller designed in this paper and to facilitate the simulation design in the next section, the adaptive NN command filtering control algorithm scheme is shown in Figure 2 and Algorithm 1. □

4. SIMULATION

In the above formulation of the paper, the research work has been completed. In this section, the simulation verification of the designed finite-time controller will be done using matlab.

Example 1: The following second-order nonlinear system is used as the simulation object:

$$\begin{cases} \dot{x}_1 = (1 + 0.1\cos(x_1))x_2 + x_1 x_2^2 + d_1(t) \\ \dot{x}_2 = u + x_2^2 \sin(x_1) + d_2(t) \\ y = x_1 \end{cases} \tag{53}$$

where $d_1(t) = 0.1\sin(0.1t)$,$d_2(t) = 0.1\sin(0.5t)$. The desired trajectory tracking signal is $y_d = 0.5\sin(1.5t)$, and the control objective is to utilize a controller u designed to enable the input to track the expected target path y_d.

The relationship between the actual input signal u and the actual control signal v of the system is defined as follows

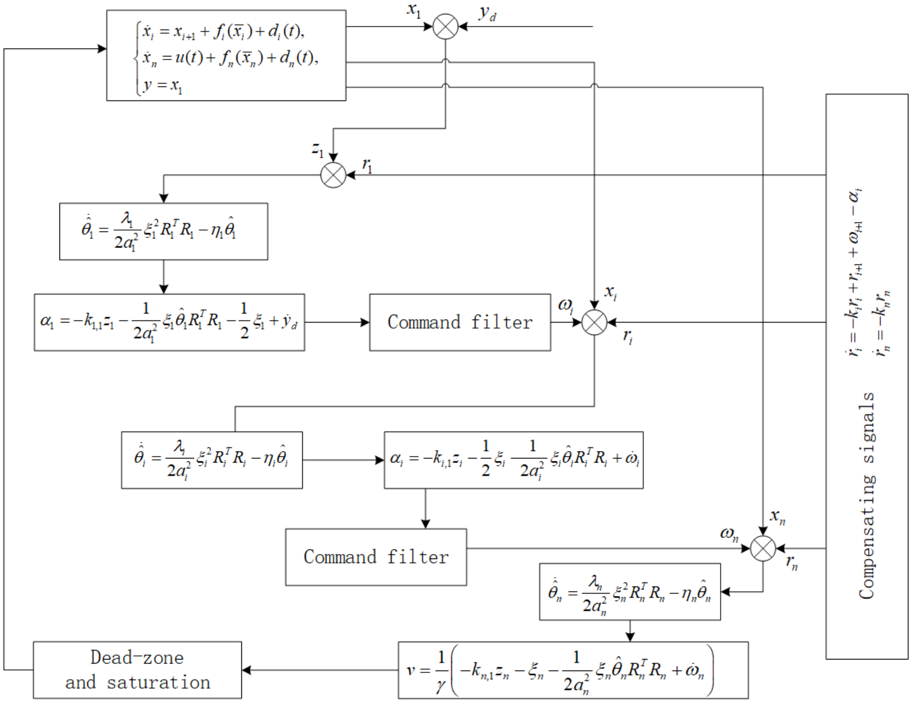

Figure 2. The block diagram of the control scheme.

$$u = \begin{cases} 20, & v > 20 \\ 0.6(v - 0.6), & 0.6 < v < 20 \\ 0, & -0.6 < v < 0.6 \\ 0.6(v + 0.6), & -20 < v < -0.6 \\ -20, & v < -20 \end{cases} \quad (54)$$

The control law, the adaptive law, and its related parameters are designed as follows: $k_1 = 10$, $k_2 = 15$, $a_1 = a_2 = 10$, $\gamma = 1$, $\omega_\tau = 60$, $\varsigma = 0.85$, $\lambda_1 = 0.5$, $\lambda_2 = 0.1$, $\eta_1 = 1$, $\eta_2 = 0.8$. The initial states and updating laws are selected as $[x_1(0), x_2(0)]^T = [0.3, 0.5]^T, [\hat{\theta}_1(0), \hat{\theta}_2(0)]^T = [0.2, 0.3]^T$.

Since RBF NNs have excellent approximation performance, they are often used as approximate models for unknown nonlinearities. In the present study, the RBF NNs are used to approximate the unknown nonlinear term $h(Z)$. The following Gaussian function is chosen as the basis function of RBF NNs, and its expression as

$$R_i(Z) = \exp(-\frac{(Z - c_i)^T (Z - c_i)}{2}) \quad (55)$$

where $i = 1, 2, \ldots, 8$, The distribution interval of the center c_i of the Gaussian function is [-1,1].

The simulation results in this example are presented in Figure 3, Figure 4, and Figure 5. Figure 4A illustrates the trajectory of the system output and reference signals. To demonstrate the effectiveness of the controller designed in this paper, the control strategy from the literature[38] is used as a comparison to plot its system

Table 1. Example 2 Parameters of a single-link robotic arm system

Parameter	Description	Value
J	torsion coefficient	$0.5\ \mathrm{kg\cdot m^2}$
M	mess of the link	1 kg
g	acceleration of gravity	$9.8\ \mathrm{m/s^2}$
l_0	length of the connecting rod	1 m
B	coefficient of friction	$0.5\ \mathrm{N/m^2}$

output tracking curve as trajectory y_c in Figure 4A. From Figure 4A, it can be seen that the control strategy designed in this paper using command filters has better tracking performance than the control strategy in the literature[38] using DSC. Figure 4B demonstrates the tracking error trajectory plots of the control strategy and the comparison control scheme in this paper. It is obvious from Figure 4 that the command filtered adaptive controller designed in this paper has better tracking performance and smaller tracking errors.

Figure 3A illustrates the trajectory of the controller signals and control inputs. After the dead zone and saturated nonlinear constraints, the amplitude of the control input becomes smaller and the input curve becomes smoother, which meets the actual needs of the real physical system. Figure 3B illustrates the trajectory of the adaptive parameters $\hat{\theta}_1, \hat{\theta}_2$. Figure 5A depicts the trajectory of the system state x_2 and the command filter output ω_2. As can be seen in Figure 5A, the command filter output avoids the computational complexity of virtual control signal derivation while completely replacing the virtual controller. The compensation signal is used to compensate for the filtering error introduced due to the command filter, the trajectory of which is depicted in Figure 5B.

Example 2: In this section, a single-link manipulator system containing stochastic perturbations is used as an example to demonstrate the effectiveness and practicality of the designed controller. The single-link manipulator system schematic is exhibited in Figure 6A. The single-link manipulator system dynamic model[39] is given as:

$$J\ddot{q} = -Mgl_0\sin(q) - B\dot{q} + u(v) \tag{56}$$

in which q, $\dot{q}$, and $\ddot{q}$ are the coordinates, velocity, and acceleration of angles, respectively. $u(v)$ is the input torque subject to saturation and deadband. Table 1 lists all the parameters of the single-link manipulator system.

We can rewrite the system (56) as follows:

$$\begin{cases} \dot{x}_1 = x_2 \\ \dot{x}_2 = 2u(v) - 19.6\sin(x_1) - x_2 - d(t) \\ y = x_1 \end{cases} \tag{57}$$

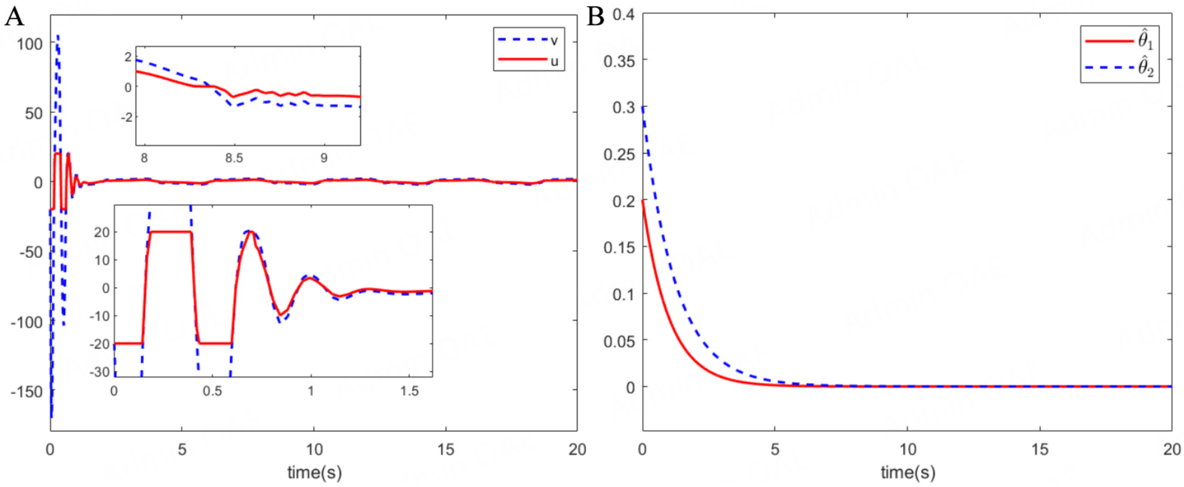

Figure 3. (A) Control input. (B) adaptive parameters.

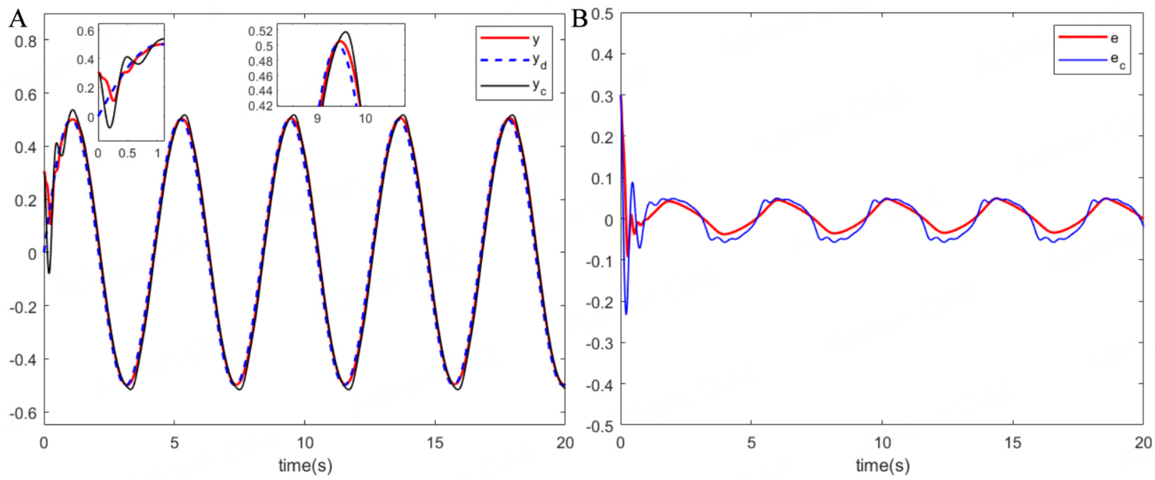

Figure 4. (A) System output and desired trajectory. (B) tracking error.

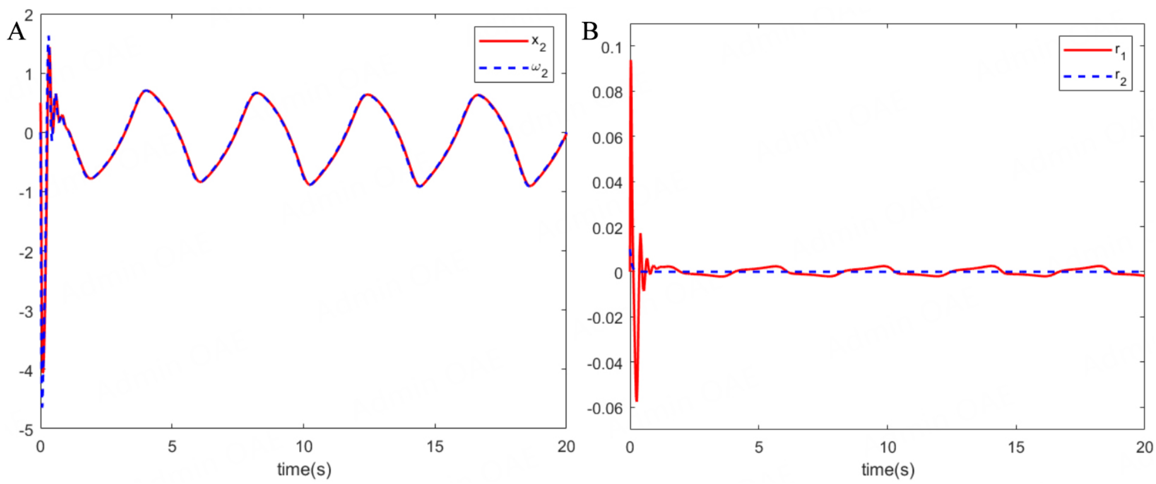

Figure 5. (A) State variable x_2 and filter output ω_2. (B) compensatory signal.

where $d(t)$ is a bounded white noise signal, which is exhibited in Figure 6B. The desired trajectory tracking signal is $y_d = 0.5\sin(t)+0.5\sin(0.5t)$. The dead zone and saturation nonlinear models are described as follows

$$u = \begin{cases} 10, & v \geq 10 \\ 0.85(v-0.6), & 0.5 < v < 10 \\ 0, & -0.5 < v < 0.5 \\ 0.85(v+0.6), & -10 < v < -0.5 \\ -10, & v \leq -10 \end{cases} \tag{58}$$

The control law, the adaptive law, and its related parameters are designed as follows: $k_1 = 15$, $k_2 = 15$, $a_1 = a_2 = 10$, $\gamma = 1$, $\omega_\tau = 60$, $\varsigma = 0.85$, $\lambda_1 = 0.5$, $\lambda_2 = 0.2$, $\eta_1 = 1$, $\eta_2 = 0.8$. The initial states and updating laws are selected as $[x_1(0), x_2(0)]^T = [0.3, 0.5]^T$,$\left[\hat{\theta}_1(0), \hat{\theta}_2(0)\right]^T = [0.15, 0.08]^T$.

The simulation results in this example are presented in Figure 6, Figure 7, and Figure 8. Figure 7A displays the trajectory of the system output and reference signals for the control scheme in this paper and the control strategy in the literature[38]. The tracking errors of the control strategies in this paper and the comparative literature are plotted in Figure 7B. Figure 7 demonstrates that the control strategy, using command filters and compensation mechanisms in this paper, has better tracking performance and smaller tracking errors. Figure 8A demonstrates the controller trajectory and the trajectory of the control input, from which it is clear that after the deadband and saturation constraints, the control input amplitude is greatly reduced while ensuring good tracking performance.

In order to demonstrate the robustness and stability of the adaptive NN tracking control algorithm proposed in this paper, perturbations $d(t) = 1.5\sin(5t)$ are added to the control input signal u. Figure 9 gives a comparison of the trajectories of the control input signal and the system output for additional disturbances and no disturbances. From the figure, it can be seen that the adaptive NN controller designed in this paper has good robustness and stability.

From the simulation results shown in this section, it is easy to see that by applying the finite-time NN tracking controller designed in this paper and choosing appropriate parameters, the system can obtain good tracking performance when all signals are bounded and the actual control inputs satisfy the deadband and saturation constraints, and the use of command filters and compensation mechanisms overcomes the problem of exploding computational complexity due to the derivation of the virtual control signals, which proves the practicability and validity of the controller we designed.

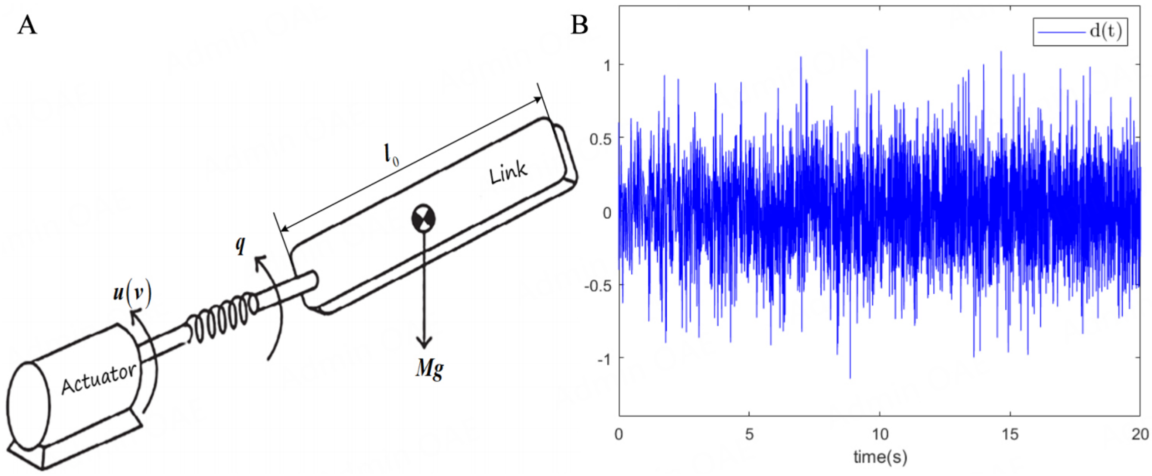

Figure 6. Example 2: (A) Single-link manipulator. (B) curves of bounded interference signals.

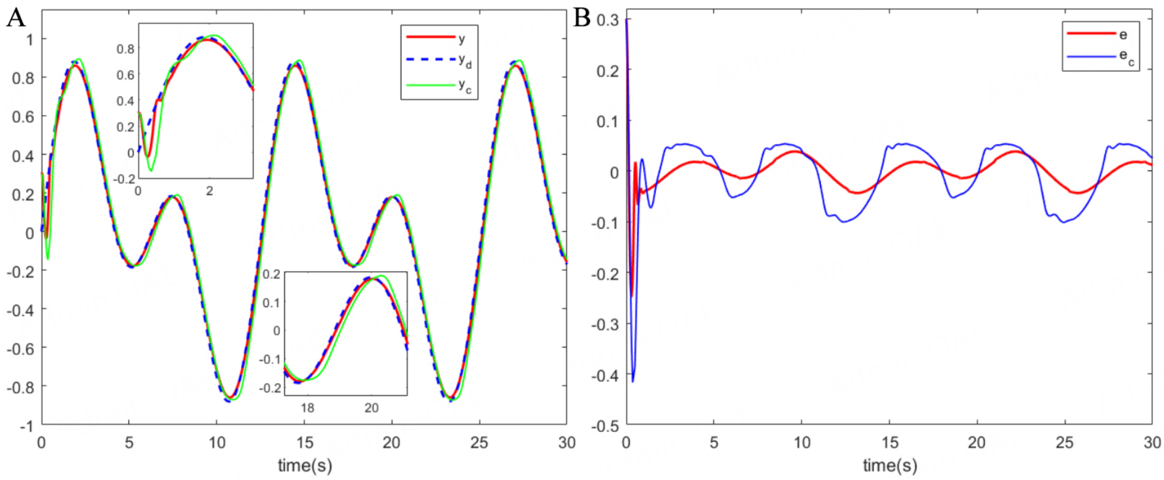

Figure 7. Example 2: (A) System output. (B) tracking error.

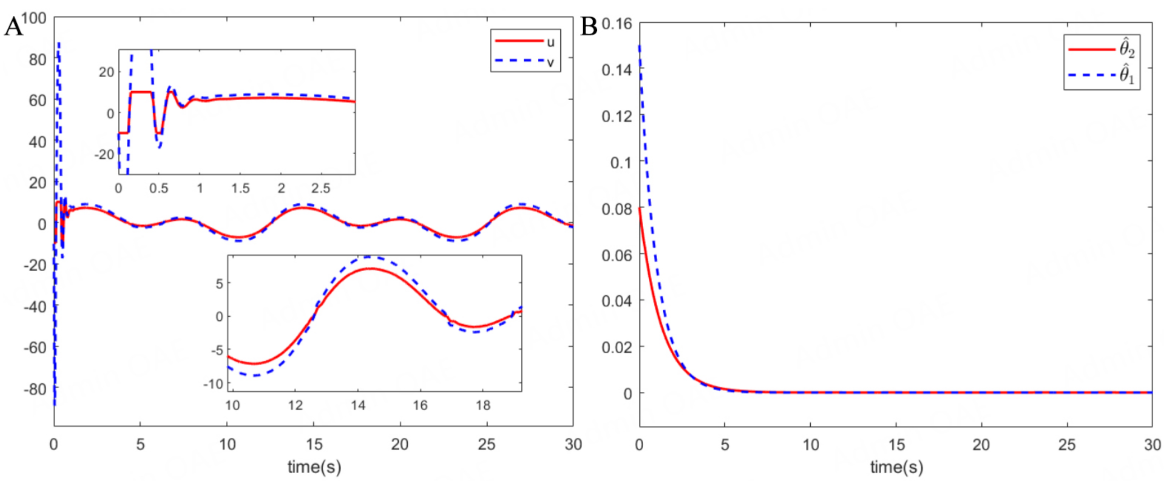

Figure 8. Example 2: (A) Control input. (B) adaptive parameters.

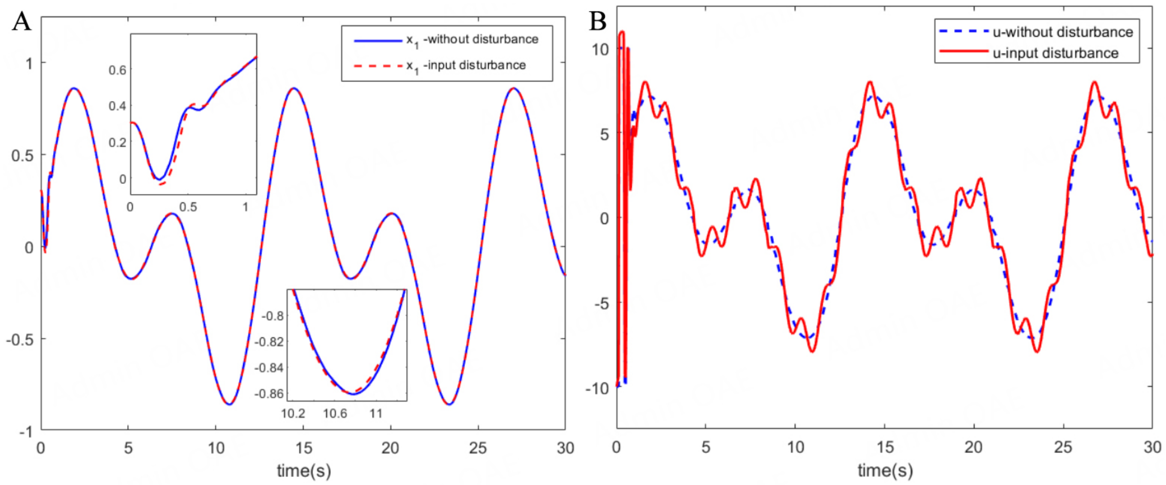

Figure 9. Example 2: system output and control input with disturbance and without disturbance.

5. CONCLUSIONS

In real production process environments, special requirements are usually imposed on system actuator inputs, such as limiting the maximum amplitude of the inputs to a certain range to ensure safe and reliable operation of the system and avoiding fluctuations of the control inputs near zero as much as possible to minimize consumption and reduce actuator losses. Deadband and saturation constraints are specific manifestations of the above problems in real physical systems, which are commonly found in many practical systems, such as unmanned aircraft systems, electromechanical systems, and robotic systems. In order to solve the effects of multi-actuator constraints and external disturbances on nonlinear systems, an adaptive NN finite time tracking controller based on command filtering is designed in this paper. The effects of dead zones and saturated nonlinear constraints on the controller design are eliminated through an equivalent transformation. Using the command filtering technique, the problem of exploding computational complexity due to virtual control signal derivatives is overcome while accomplishing the virtual controller control task. The controller can guarantee the boundedness of all signals in the controlled system, and the output of the system can quickly track the desired reference trajectory. Simulation results verify the effectiveness and rationality of the designed control strategy.

DECLARATIONS

Acknowledgments

Special thanks to the School of Information and Control Engineering, Qingdao University of Technology, China, for providing technical support for this research.

Authors' contributions

Made substantial contributions to the conception and design of the study and performed validation analysis and interpretation: Li Y (Li Yinguang), Zhang J

Provided simulation design and administrative and technical support: Li Y (Li Yang)

Financial support and sponsorship

This work was supported in part by the National Natural Science Foundation (62203247) from China.

Availability of data and materials
Not applicable.

Conflicts of interest
All authors declared that there are no conflicts of interest.

Ethical approval and consent to participate
Not applicable.

Consent for publication
Not applicable.

Copyright

REFERENCES

1. Yin X, Zhang Q. Backstepping-based state estimation for a class of stochastic nonlinear systems. *Complex Eng Syst* 2022;2:1. DOI
2. Liu Q, Cai Z, Chen J, Jiang B. Observer-based integral sliding mode control of nonlinear systems with application to single-link flexible joint robotics. *Complex Eng Syst* 2021;1:8. DOI
3. Li Y, Zhu Q, Zhang J. Distributed adaptive fixed-time neural networks control for nonaffine nonlinear multiagent systems. *Sci Rep* 2022;12:8459. DOI
4. Chen M, Wang H, Liu X. Adaptive fuzzy practical fixed-time tracking control of nonlinear systems. *IEEE Trans Fuzzy Syst* 2021;29:664–73. DOI
5. Kanellakopoulos I, Kokotovic PV, Morse AS. Systematic design of adaptive controllers for feedback linearizable systems. In: 1991 American Control Conference; Boston, MA, USA, 26-28 June 1991. pp. 649–54. DOI
6. Ba D, Li YX, Tong S. Fixed-time adaptive neural tracking control for a class of uncertain nonstrict nonlinear systems. *Neurocomputing* 2019;363:273–80. DOI
7. Wang F, You Z, Liu Z, Chen CLP. A fast finite-time neural network control of stochastic nonlinear systems. *IEEE Trans Neural Netw Learn Syst* 2023;34:7443–52. DOI
8. He W, Mu X, Zhang L, Zou Y. Modeling and trajectory tracking control for flapping-wing micro aerial vehicles. *IEEE/CAA J Automat Sin* 2021;8:148–56. DOI
9. Dong H, Yang X. Adaptive neural finite-time control for space circumnavigation mission with uncertain input constraints. *J Franklin Inst* 2021;358:3353–75. DOI
10. Cui D, Zou W, Guo J, Xiang Z. Adaptive fault-tolerant decentralized tracking control of switched stochastic uncertain nonlinear systems with time-varying delay. *Int J Adapt Control Signal Process* 2022;36:2971–87. DOI
11. Ha M, Wang D, Liu D. Discounted iterative adaptive critic designs with novel stability analysis for tracking control. *IEEE/CAA J Automat Sin* 2022;9:1262–72. DOI
12. Lv Y, Fu J, Wen G, Huang T, Yu X. Distributed adaptive observer-based control for output consensus of heterogeneous mass with input saturation constraint. *IEEE Trans Circuits Syst I Regul Pap* 2020;67:995–1007. DOI
13. Liu Z, Han Z, Zhao Z, He W. Modeling and adaptive control for a spatial flexible spacecraft with unknown actuator failures. *Sci China Inf Sci* 2021;64:152208. DOI
14. Tong S, Li Y. Adaptive fuzzy output feedback tracking backstepping control of strict-feedback nonlinear systems with unknown dead zones. *IEEE Trans Fuzzy Syst* 2012;20:168–80. DOI
15. Li Y, Liu L, Feng G. Robust adaptive output feedback control to a class of non-triangular stochastic nonlinear systems. *Automatica* 2018;89:325–32. DOI
16. Li YX. Finite time command filtered adaptive fault tolerant control for a class of uncertain nonlinear systems. *Automatica* 2019;106:117–23. DOI
17. Sui S, Chen CLP, Tong S. Fuzzy adaptive finite-time control design for nontriangular stochastic nonlinear systems. *IEEE Trans Fuzzy Syst* 2019;27:172–84. DOI
18. Lu C, Pan Y, Liu Y, Li H. Adaptive fuzzy finite-time fault-tolerant control of nonlinear systems with state constraints and input quantization. *Int J Adapt Control Signal Proces* 2020;34:1199–219. DOI
19. Yu J, Cheng S, Shi P, Lin C. Command-filtered neuroadaptive output-feedback control for stochastic nonlinear systems with input constraint. *IEEE Trans Cybern* 2023;53:2301–10. DOI
20. Li YX. Command filter adaptive asymptotic tracking of uncertain nonlinear systems with time-varying parameters and disturbances. *IEEE Trans Automat Contr* 2022;67:2973–80. DOI
21. Shi X, Lim CC, Shi P, Xu S. Adaptive neural dynamic surface control for nonstrict-feedback systems with output dead zone. *IEEE Trans*

Neural Netw Learn Syst 2018;29:5200–13. DOI
22. Zhao S, Pan Y, Du P, Liang H. Adaptive control for non-affine nonlinear systems with input saturation and output dead zone. *Appl Math Comput* 2020;386:125506. DOI
23. Wang L, Wang H, Liu PX, Ling S, Liu S. Fuzzy finite-time command filtering output feedback control of nonlinear systems. *IEEE Trans Fuzzy Syst* 2022;30:97–107. DOI
24. Yu J, Shi P, Dong W, Lin C. Adaptive fuzzy control of nonlinear systems with unknown dead zones based on command filtering. *IEEE Trans Fuzzy Syst* 2018;26:46–55. DOI
25. Yu H, Yu J, Wang QG, Lin C. Time-varying BLFs-based adaptive neural network finite-time command-filtered control for nonlinear systems. *IEEE Trans Syst Man Cybern Syst* 2023;53:4696–704. DOI
26. Zhang J, Jiang Y, Li X, Luo H, Yin S, Kaynak O. Remaining useful life prediction of lithium-ion battery with adaptive noise estimation and capacity regeneration detection. *IEEE/ASME Trans Mechatron* 2023;28:632–43. DOI
27. Zhao L, Yu J, Wang QG. Finite-time tracking control for nonlinear systems via adaptive neural output feedback and command filtered backstepping. *IEEE Trans Neural Netw Learn Syst* 2021;32:1474–85. DOI
28. Li Y, Yang T, Tong S. Adaptive neural networks finite-time optimal control for a class of nonlinear systems. *IEEE Trans Neural Netw Learn Syst* 2020;31:4451–60. DOI
29. Li H, Zhao S, He W, Lu R. Adaptive finite-time tracking control of full state constrained nonlinear systems with dead-zone. *Automatica* 2019;100:99–107. DOI
30. Liu J, Wang C, Li X, Cai X. Adaptive finite-time practical consensus protocols for second-order multiagent systems with nonsymmetric input dead zone and uncertain dynamics. *J Franklin Inst* 2019;356:3217–44. DOI
31. Wang J, Zhang H, Ma K, Liu Z, Chen CLP. Neural adaptive self-triggered control for uncertain nonlinear systems with input hysteresis. *IEEE Trans Neural Netw Learn Syst* 2022;33:6206–14. DOI
32. Liu Y, Chen Y. Dynamic memory event-triggered adaptive control for a class of strict-feedback nonlinear systems. *IEEE Trans Circuits Syst II Express Briefs* 2022;69:3470–74. DOI
33. Wang H, Kang S, Zhao X, Xu N, Li T. Command filter-based adaptive neural control design for nonstrict-feedback nonlinear systems with multiple actuator constraints. *IEEE Trans Cybern* 2022;52:12561–70. DOI
34. Chen M, Wang H, Liu X. Adaptive practical fixed-time tracking control with prescribed boundary constraints. *IEEE Trans Circuits Syst I Regul Pap* 2021;68:1716–26. DOI
35. Yuan X, Chen B, Lin C. Neural adaptive fixed-time control for nonlinear systems with full-state constraints. *IEEE Trans Cybern* 2023;53:3048–59. DOI
36. Farrell JA, Polycarpou M, Sharma M, Dong W. Command filtered backstepping. *IEEE Trans Automat Contr* 2009;54:1391–95. DOI
37. Liang Y, Li YX, Hou Z. Adaptive fixed-time tracking control for stochastic pure-feedback nonlinear systems. *Int J Adapt Control Signal Process* 2021;35:1712–31. DOI
38. Wang H, Xu K, Liu PX, Qiao J. Adaptive fuzzy fast finite-time dynamic surface tracking control for nonlinear systems. *IEEE Trans Circuits Syst I Regul Pap* 2021;68:4337–48. DOI
39. Xu B, Li YX, Tong S. Neural learning fixed-time adaptive tracking control of complex stochastic constraint nonlinear systems. *J Franklin Inst* 2023;360:13671–91. DOI